


Event activity measurements and mid-rapidity correlations in 200 GeV p+Au collisions at STAR[†]

David Stewart ¹  for the STAR Collaboration

¹ Yale University; david.j.stewart@yale.edu

[†] Presented at Hot Quarks 2018 - Workshop for young scientists on the physics of ultrarelativistic nucleus-nucleus collisions, Texel, The Netherlands, September 7-14 2018

Version November 6, 2018 submitted to Proceedings

Abstract: These proceedings report preliminary measurements of correlations between mid-rapidity charged tracks and high-rapidity event activity (EA) at STAR for $\sqrt{s_{NN}} = 200$ GeV p+Au collisions taken in 2015. These correlations are intriguing because they inform current debate over use of the Glauber model in “small” systems (here meaning p+A or d+A and denoted as “s+A”) and have implications for calculating nuclear modification and quenching observables in these systems. The results support concerns about centrality binning in p+Au collisions, and as such motivate using ratios of semi-inclusive, as opposed to fully inclusive, jet spectra to look for jet enhancement or suppression.

Keywords: STAR; jet; p+Au; RAA; suppression; small systems; 200GeV; Ncoll; event activity

1. Introduction

The statistical distributions of binary nucleon-nucleon collisions in A+A collisions (N_{coll}), calculated by the Glauber Model [1], as a function of impact parameter b , play an important role in probing nuclear modification in A+A collisions. The N_{coll} distributions are binned into centrality classes. In each distribution, N_{coll} is maximum for the most central bin, i.e. with $b \rightarrow 0$, and decreases monotonically through the most peripheral bin. The results of hard scatterings are compared in ratio to those from p+p collisions scaled by N_{coll} . For jets, the deviation of this ratio (R_{AA}^{jet}) from unity is an indication of nuclear modification. In A+A events, the strong suppression of R_{AA}^{jet} is an indicator of quark gluon plasma, QGP, formation. The traditional assumption was that small systems would not form a QGP. Therefore, R_{sA}^{jet} was measured in order to study cold nuclear matter effects.

The first inclusive measurements of R_{sA}^{jet} were reported for 5.02 TeV p+Pb collisions at the LHC by ALICE [2], CMS [3], and ATLAS [4], and for 200 GeV d+Au collisions at PHENIX at RHIC [5]. As expected, the values of R_{sA}^{jet} , when not binned into centrality classes, were consistent with unity. However, centrality binned R_{sA}^{jet} showed significant suppression/enhancement for central/peripheral collisions at both ATLAS and PHENIX, a similar result to that interpreted as a QGP signal in A+A collisions. Tantalizingly, this coincided with larger community interest in small systems as a variety of particle collectivity signals were observed in s+A collisions.

2. Event activity estimation and correlations to R_{sA}^{jet}

Calculating R_{AA}^{jet} assumes that the probability of a hard scattering scales linearly with N_{coll} , which is applied to collisions by assuming that it scales monotonically with a measured event activity estimation (EA_{est}). In the above measurements, EA_{est} values were determined by detectors at η values outside of the region where the jets were reconstructed in order to avoid auto-correlations between EA_{est} and R_{sA}^{jet} .

33 The observed suppression/enhancement of R_{sA}^{jet} may artificially result from difficulties applying
 34 N_{coll} which are unique to small systems. First, compared to A+A collisions, small systems have large
 35 fluctuations in EA_{est} coupled with a relatively limited range of N_{coll} . This can result in a dynamical bias
 36 when calculating R_{sA}^{jet} [6]. More intriguing is the possibility that individual nucleon-nucleon collisions
 37 within a single s+A collision that share a common nucleon are not independent. The effects of such a
 38 correlation would be strongly evident in a p+A collision relative to an A+A collision. In the former,
 39 every nucleon-nucleon collision shares the same proton; in the latter many independent sets of such
 40 collisions would be superimposed, thereby masking the effects of the correlation.

41 A study of p+Pb collisions at LHC energies concluded that a 20% suppression of soft particles
 42 correlated with the presence of a hard scattering would reproduce the enhancement/suppression
 43 observed in R_{sA}^{jet} [7]. Energy conservation of a proton (or deuteron) common to a set of nucleon-nucleon
 44 collisions may provide the physics mechanism for this correlation. Jet production would require a
 45 hard scattering in one nucleon-nucleon collision, and therefore a reduction in energy available for the
 46 production of soft particles in the remaining collisions. Two such theory calculations found this to be a
 47 sufficient explanation for the observed suppression of central R_{sA}^{jet} , one of which also found it sufficient
 48 for the peripheral enhancement [8][9].

49 3. Correlations of EA_{est} to mid-rapidity charged tracks at STAR for p+Au collisions

50 STAR has a large set of $\sqrt{s_{\text{NN}}} = 200$ GeV p+Au collisions recorded in 2015 which will help address
 51 questions raised by the jet measurements already released by PHENIX and the LHC experiments.
 52 Measurements of mid-rapidity charged track correlations to high- η EA_{est} , presented in Figure 1 and
 53 Figure 2, clearly indicate that further study is required prior to calculating the R_{sA}^{jet} .

54 The figures present data from events with two separate triggers. First: minimum bias (MB)
 55 events. Second: events triggered by the electromagnetic calorimeter (EMC) selected by the hit with the
 56 maximum transverse energy (E_T^{trig}). The correlations reported are for charged tracks measured in the
 57 time projection chamber (TPC) which has good track resolution from 0.2 to 30 GeV/c and has, as does
 58 the EMC, full azimuthal coverage. EA_{est} is measured as the sum of the signal in the inner ring of the
 59 beam beam counter (BBC) in the Au-going direction. The BBC consists of sets of plastic scintillators
 60 arrayed around the beam pipe; the inner ring of which covers rapidity range 3.3 to 5.8.

61 These preliminary results are detector level and uncorrected for detector acceptance or inefficiency
 62 effects. However, the conclusions presented depend on the data's monotonicity and relative
 63 distributions and are consequently not sensitive to detector tracking efficiencies and pileup. Statistical
 64 uncertainties are plotted for all data. Additionally, a small relative trigger bias is added in quadrature
 65 with the statistical uncertainty in Figure 2 (a2), (b), and (c). This bias is quantified by the difference in
 66 results from the MB data when cut for EMC hits so as to mimic the EMC trigger and the results from
 67 the actual EMC triggered data.

68 Figure 1 (a) shows the EA_{est} distributions for MB events (on left) and EMC triggered events
 69 (on right). As in the case of centrality in Glauber calculations, EA_{est} percentiles are defined by the
 70 MB distribution with 100% being the lowest and 0% the highest value. Here the EA distribution is
 71 divided into low (100-70%), medium (30-70%), and high (0-30%) activity bins. For each EA_{est} bin, the
 72 distribution of multiplicity, summed p_T , and maximum single track p_T , are given in (b), (c), and (d).
 73 Compared to A+A collisions, the distributions in p+Au collisions heavily overlap among EA_{est} bins.
 74 As expected, the mean values of multiplicity and summed track p_T are higher for the high EA_{est} bins.
 75 The normalization of the curves in (d) is dominated by the first few, low- p_T , bins. In these bins the
 76 spectra from high, medium, and low EA_{est} events are fairly comparable. After these low p_T bins, the
 77 spectrum of each EA_{est} bin continues to be roughly equivalent for harder scatterings in the MB data;
 78 however, for the EMC triggered data, the high EA_{est} bin's spectrum is somewhat suppressed relative
 79 to the low EA_{est} bin's spectrum.

80 Figure 2 (a1) gives the same EA_{est} distributions (MB and EMC triggered) shown in Figure 1 (a).
 81 The EA_{est} binning, consistent between all plots, is selected for uniform numbers of MB events. The

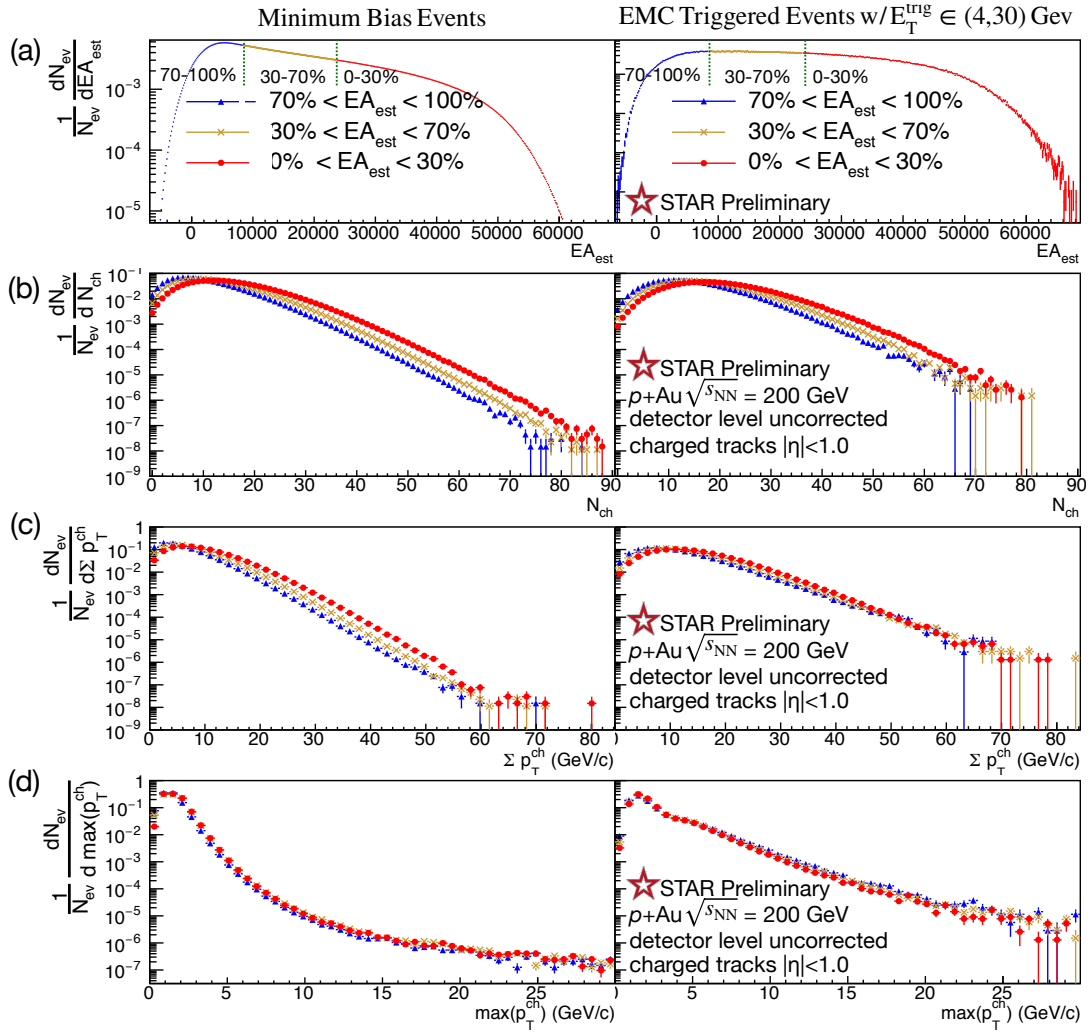


Figure 1. Correlations between charged tracks at STAR ($|\eta| < 1$) and EA_{est} , the Au-going BBC inner ring signal ($|\eta| \in (3.3, 5.8)$). (a) left: EA_{est} distribution of MB events, binned for the maximum and minimum 30% as well as the middle 40% of events. (a) right: distribution of EA_{est} in for EMC triggered events; the binning boundaries and labels are determined by the MB distribution. Columns (b), (c), and (d) give the distributions for the low, mid, and high EA_{est} bins for charged track multiplicity, summed p_T , and maximum p_T respectively.

82 remaining panels plot average (a2) (normalized) number of events, (b) multiplicity, (c) summed track
 83 p_T , and (d) maximum single track p_T . The results of two subsets of the EMC data, with higher trigger
 84 thresholds, are also plotted. The most striking results are deviations from what would result if EA_{est}
 85 and N_{coll} scaled positively, monotonically, together. If true, that scaling would result in correlations in
 86 (a2)-(d) that are: (1) positive, except, of course, for MB events in (a2), and, (2) smallest for MB events
 87 and successively larger for EMC triggered events with successively higher trigger thresholds. Instead,
 88 while each correlation is positive in (a2), the correlations are smaller for each successively higher E_T^{trig}
 89 threshold; the data is too limited for harder triggers to see if there would be an actual turnover at a
 90 sufficiently high threshold. Correlations in (c) and (d) are about as naively expected, although it is
 91 curious that mean multiplicity and summed p_T appear relatively saturated by the time there is an
 92 8 GeV E_T^{trig} such that they increase only slightly with the higher 12 GeV threshold. Most notably, each
 93 EMC triggered distribution (d) is anti-correlated; this directly contradicts the assumption that hard
 94 scatterings (and therefore naively higher E_T^{trig} values) scale linearly with EA_{est} .

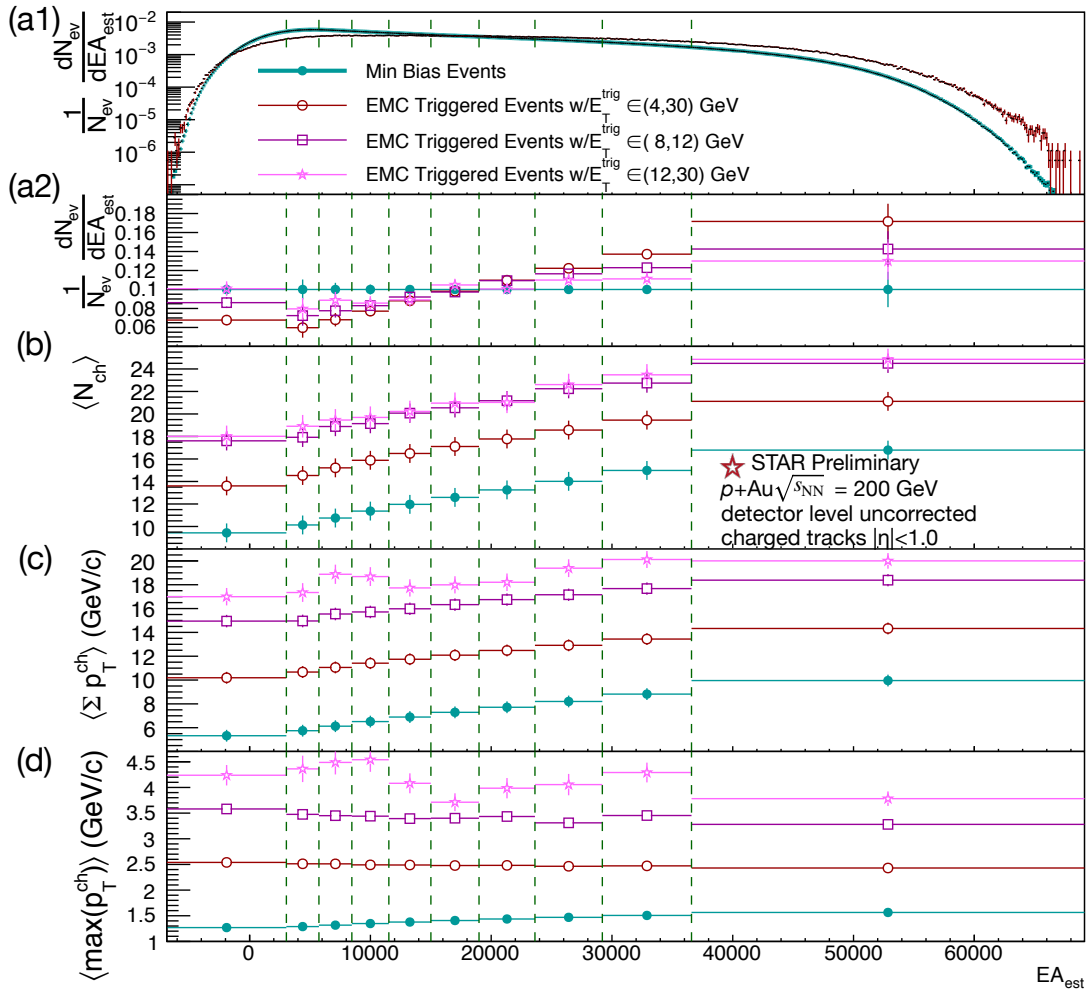


Figure 2. Correlations between charged tracks at STAR ($|\eta| < 1$) and EA_{est} , the Au-going BBC inner ring signal ($|\eta| \in (3.3, 5.8)$). Each panel is plotted with data from MB events as well EMC E_T^{trig} triggered events. (a) The number of events of each BBC bin; each bin's boundaries are selected to contain 10% of the MB data. (b) Average number of charged tracks per event. (c) Average sum of p_T per event. (d) Average maximum track p_T per event.

95 4. Summary

96 Correlations of mid rapidity charged track observables to high η EA_{est} have been presented. The
 97 results imply challenges to the use of EA_{est} to determine associated N_{coll} values. These difficulties
 98 motivate the use of semi-inclusive jet spectra, in which N_{coll} cancels in the ratio, instead of fully
 99 inclusive spectra, to probe for jet suppression/enhancement in p+Au collisions [10][11].

100 **Funding:** This research was funded by U.S. Department of Energy under grant number DE-SC004168.

101 References

- 102 1. G. David, PoS **INPC2016**, 345 (2017).
- 103 2. J. Adam et al. (ALICE), Eur. Phys. J. **C76**, 271 (2016).
- 104 3. V. Khachatryan et al. (CMS), Eur. Phys. J. **C76**, 372 (2016).
- 105 4. G. Aad et al. (ATLAS), Phys. Lett. **B748**, 392 (2015).
- 106 5. A. Adare et al. (PHENIX), Phys. Rev. Lett. **116**, 122301 (2016).
- 107 6. J. Adam et al. (ALICE), Phys. Rev. **C91**, 064905 (2015).
- 108 7. A. Bzdak, V. Skokov, and S. Bathe, Phys. Rev. **C93**, 044901 (2016).

- 109 8. N. Armesto, D. C. Gülhan, and J. G. Milhano, *Phys. Lett.* **B747**, 441 (2015).
110 9. M. Kordell and A. Majumder, *Phys. Rev.* **C97**, 054904 (2018).
111 10. S. Acharya et al. (ALICE), *Phys. Lett.* **B783**, 95 (2018).
112 11. L. Adamczyk et al. (STAR), *Phys. Rev.* **C96**, 024905 (2017).

113 © 2018 by the author. Submitted to *Proceedings* for possible open access publication
114 under the terms and conditions of the Creative Commons Attribution (CC BY) license
115 (<http://creativecommons.org/licenses/by/4.0/>).